PHYSICAL REVIEW B VOLUME 19, NUMBER 4 15 FEBRUARY 1979

Effect of edge anomaly on the valence-band Auger spectra of metals

Pierre Longe
Institut de Physique, Université de Liège, Sart-Tilman, B-4000 Liège, Belgium

Shyamalendu M. Bose
Department of Physics and Atmospheric Science, Drexel University, Philadelphia, Pennsylvania 19104
(Received 5 June 1978)

The processes responsible for the anomalous edge behavior in the x-ray band spectra of metals are found to play important roles in modifying the intensity of *CVV* Auger-electron emission spectra. The dynamical effects related to the sudden switching of the core-hole potential are known to produce a power-law behavior in the neighborhood of the upper emission edge. Using simplified diagrams and a realistic pseudopotential for the core-hole interaction, we have extended the edge theory to energies well below the Auger emission edge. A significant shift in the position of the maximum of the $L_{23}VV$ Auger emission intensity of Al is calculated.

I. INTRODUCTION

The effect of excitations of weak-energy electron-hole pairs on the x-ray band spectra of metals was first investigated by Mahan[1] and Nozières and deDominicis[2] (ND). It was found that such excitations were responsible for the anomalous behavior of the soft-x-ray spectra of metals very near the emission or the absorption edge. The theory was also applied to the case of the photoemission spectra of metals by Doniach and Šunjić.[3] Natta and Joyes[4] (NJ) then studied the weak-energy pair-excitation effect on the core-valence-valence (*CVV*) Auger spectra of metals. By a direct application of the ND theory to the Auger case, these authors showed that very close to the emission edge the Auger intensity was also given by a power law with the exponent

$$\alpha^A = 2(2\delta_0/\pi) + \sigma - 1 , \tag{1}$$

with

$$\sigma = -2 \sum_{l=0}^{\infty} (2l+1)\left(\frac{\delta_l}{\pi}\right)^2 , \tag{2}$$

where, as in ND theory, δ_l's are the phase shifts of the Fermi-level electrons scattered by the initial bound core hole.

In the case of x-ray band spectra, the power-law exponent was found to be[2]

$$\alpha_l^X = 2\delta_l/\pi + \sigma . \tag{3}$$

Let us note that in the Auger exponent (1), only the $l=0$ contribution is retained. This is reasonable because of the short-range character of the Auger collision in which a large momentum is transferred to the ejected electron. The exponent for the x-ray spectra depends sensitively on the symmetry of the core level, i.e., the l value depends on the nature of the x-ray transition and is controlled by the optical selection rule. Numerical computations[5,6] of the exponent α_l^X have shown that for the L spectra the intensity is singular at the emission and absorption edges, whereas it remains finite in the edge region for the K spectra.

The two exponents (1) and (3) differ in two important respects: α^A has an extra factor of 2 in the first term, and it also has an additional third term -1. The first terms of both Eqs. (1) and (3) are related to the open-line part of the ND problem. The additional factor of 2 in Eq. (1) appears because in a *CVV* Auger process two conduction electrons participate, whereas in the x-ray process only one such electron is involved. Indeed, in the Auger collision a conduction electron drops into a previously ionized core level (as in the x-ray emission process), while another is ejected out of the metal as an Auger electron. The term σ in Eqs. (1) and (3) is related to Anderson orthogonality (closed-loop part of the ND problem) and is the same in both Auger and x-ray processes. In the zero-order theory, the *CVV* Auger band is obtained from the self-convolution of a state density function having a sharp edge at the Fermi level (step function). This self-convolution is responsible for the occurrence of the third term in Eq. (1). This term -1 therefore, appears in the zero-order theory and it is not to be related to the weak-energy pair excitations in the metal. Because of the presence of this term, the Auger-band intensity drops off smoothly at the upper edge.

It is thus practically impossible to measure the effects of the NJ power law in the edge region of the Auger spectra. First, α^A is always *negative*, and as such, unlike the x-ray case (L bands), no spike is expected to occur in the edge region. Second, the slope of the emission intensity at the upper edge is modified by the NJ theory, but this slope cannot be measured experimentally since the *absolute intensity* of the observed Auger spectra is not known.

However, the scattering of the weak-energy electron-hole pair by the initial core hole, modifies the Auger line shape not only in the edge region (ND-NJ effect) but also at energies well below the emission edge. In particular, it should produce a displacement in the position of the Auger intensity maximum. Such changes in the Auger line shape and in the position of the intensity maximum have been observed experimentally.[7,8] Thus, it will be interesting to extend the ND-NJ edge theories below the edge region to calculate this displacement. However, due to inherent assumptions, these two theories are valid only very close to the edge. In this paper such an extended theory is presented for the Auger-band spectra.

The simplest, and probably a rather naive way to extend the edge theory, is to multiply the *zero*-order band intensity by the NJ power-law factor. This factor is

$$(\xi_0/\epsilon)^{\alpha A+1} ,$$

where ξ_0 is a *constant* energy which has already appeared in ND and NJ, and is estimated to be on the order of the Fermi-energy ϵ_0. (Energy $-\epsilon = \omega - 2\epsilon_0$ is the spectral energy measured from the upper edge and ω is the same energy measured from the bottom of the zero-order Auger band.) This yields an Auger-band shape whose maximum is much closer to the upper edge than that of the zero-order band shape (see dotted curve in Fig. 4). But since the ND and NJ theories are valid only for vanishing ϵ, such an extension of their results to lower energies is obviously not reliable. A proper extension of the ND edge theory for the x-ray band spectra was made by one of the authors (P. L.).[6] We will follow the same procedure for obtaining a proper theory for studying the effect of weak pair creation on the Auger-band spectra.

In Sec. II we give a general formulation of the Auger problem in terms of an appropriate Hamiltonian in which we introduce a realistic nonseparable potential, used throughout the calculation. Auger intensity is expressed in terms of Feynman diagrams which are depicted in terms of "closed-loop" parts and "open-line" parts. In Sec. III we consider the closed-loop part of the problem and obtain the appropriate exponent in terms of Born-approximation phase shifts. In Sec. IV we treat the open-line part of the problem. Numerical calculations are performed by using an appropriate pseudopotential. We present our numerical results for the $L_{23}VV$ Auger spectrum of Al in Sec. V, and conclude with a discussion.

II. FORMULATION OF THE PROBLEM

The total Hamiltonian of the system is represented by

$$H^{\text{tot}} = H_0 + H' + H_k , \tag{4a}$$

with

$$H_0 = \sum_{\underset{\sim}{p}} \epsilon_p a^\dagger_{\underset{\sim}{p}} a_{\underset{\sim}{p}} + \epsilon_B a^\dagger_B a_B + \epsilon_k a^\dagger_{\underset{\sim}{k}} a_{\underset{\sim}{k}} , \tag{4b}$$

$$H' = \sum_{\underset{\sim}{p},\underset{\sim}{p}'} V_{\vec{p}\vec{p}'} a^\dagger_B a^\dagger_{\underset{\sim}{p}} a_B a_{\underset{\sim}{p}'} , \tag{4c}$$

$$H_k = \sum_{\underset{\sim}{p},\underset{\sim}{p}'} W_{\vec{k}\vec{p}\vec{p}'} a^\dagger_B a^\dagger_{\underset{\sim}{k}} a_{\underset{\sim}{p}} a_{\underset{\sim}{p}'} + \text{c.c.} . \tag{4d}$$

The first term H_0 describes a noninteracting system where the individual states are the conduction states $\underset{\sim}{p}$, with energy $\epsilon_p = p^2/2m$, a core state B with energy ϵ_B (negative) and an Auger state $\vec{k}$; the energy of the Auger electron, $\epsilon_k = k^2/2m$, is such that it can leave the metal. The second term H' describes the interaction of the conduction electrons with the core hole. This scattering of the conduction electrons by the core hole will be treated by an infinite-order perturbative expansion (many-body expansion). The scattering potential $V_{\vec{p}\vec{p}'}$ is an effective electron-electron potential which can be written in the form

$$V_{\vec{p}\vec{p}'} = V(q) = V_{\text{ps}}(q)/\varepsilon(q) , \tag{5}$$

with $q = |\vec{p} - \vec{p}'|$ and $\varepsilon(q)$ is the static Lindhard dielectric function. This function is related to the screening effect of the conduction electrons, and $V_{\text{ps}}(q)$ is a Coulomb pseudopotential related to the Bloch wave and the core-hole structure. The pseudopotential used in this calculation is discussed in the Appendix [see Eq. (A8)]. We neglect the interaction of the outgoing Auger electron with the core hole, since this electron is fast and has little chance of interacting significantly with the localized core hole. Also, the interactions among the electrons and holes within the conduction band do not play any significant role in modifying the intensity of the Auger spectra in the *high-energy region,* in which we are mainly interested in this paper.[9] Thus we neglect these interactions as well as the dynamic part of the interaction potential (5). The last term H_k describes the interaction Hamiltonian for the Auger transition. The transition matrix element $W_{\vec{k}\vec{p}\vec{p}'}$ has a rather complicated structure since the wavelength of the Auger electron is of the order of the core radius. However, we note that the range of variation of ϵ_k is only twice the Fermi energy ϵ_0 which is small compared to the magnitude of ϵ_k. Also since ϵ_k is much greater than ϵ_p and $\epsilon_{p'}$, the $(\vec{k}, \vec{p}, \vec{p}')$ dependence of $W_{\vec{k}\vec{p}\vec{p}'}$ can be neglected, and like many other authors[4,10,11] we replace it by a constant

$$W_{\vec{k}\vec{p}\vec{p}'} = W. \tag{6}$$

Since we are interested in calculating the linear response of our system described by the Hamiltonian $H = H_0 + H'$ to the perturbation H_k we will treat H_k in the first-order perturbative expansion. Initially our system has a hole in the core state. Thus the initial state Φ_B corresponds to the ground state of an electron gas in the presence of an impurity (the core hole). In the final state the core level is occupied and there are two electrons missing from the conduction band. The Auger intensity is given by the response function

$$I(\omega) = \frac{1}{\pi} \operatorname{Re} \int_0^\infty ds\, e^{-i\omega s} \mathfrak{F}(s) , \tag{7}$$

where

$$\omega = \epsilon_k + \epsilon_B$$

and

$$\mathfrak{F}(s) = \langle \tilde{\Phi}_B | \tilde{H}_k(s) \tilde{H}_k(0) | \tilde{\Phi}_B \rangle$$

in the Heisenberg picture, or

$$\mathfrak{F}(s) = \frac{\langle \Phi_B | U(\infty, s) H_k(s) U(s,0) H_k(0) U(0, -\infty) | \Phi_B \rangle}{\langle \Phi_B | U(\infty, -\infty) | \Phi_B \rangle} \tag{8}$$

in the interaction picture.

Our model is quite similar to that of ND and NJ, although there exist two important differences which should be emphasized. The first and the essential difference between the two models is that we use the realistic *nonseparable* potential (5) for the core-hole interaction, instead of a separable one used by ND-NJ. Such a realistic potential is necessary to extend their theory beyond the edge region. The second difference is more formal and, in fact, can be seen to occur as a consequence of the first one. In the present paper we consider that the perturbation H' acts at times $t < 0$ and $t > s$, whereas in the ND-NJ model it acts at $0 < t < s$; in their model the unperturbed Hamiltonian is $H_0 + H'$ and the perturbation is $-H'$. This difference allows us to express $\mathfrak{F}(s)$ by Eq. (8), where the individual electronic states $\vec{p}$ can be described by plane waves instead of the scattered waves of ND-NJ model.

The correlation function $\mathfrak{F}(s)$ can be represented by diagrams of the type shown in Fig. 1. The Auger interactions H_k take place at times 0 and s, and are given by the white dots. The n black dots (in a diagram of order n) are related to the scattering of the conduction electrons by the core hole. As shown in Fig. 1, a general diagram typically contains two open lines A and B and a closed-loop

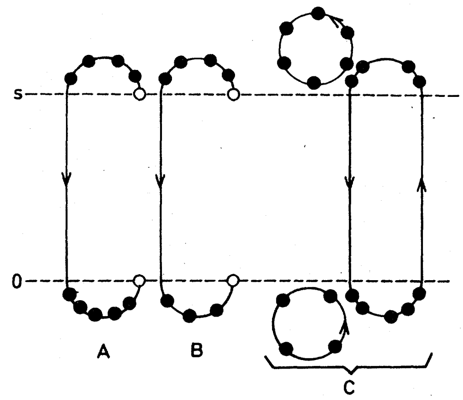

FIG. 1. Diagrammatic representation of a typical Auger process. The white dots correspond to Auger interactions at times 0 and s. The black dots represent interactions of the core hole with the conduction electrons.

part C which may, in fact, contain an unlimited number of closed loops. Such a diagram (Fig. 1) really corresponds to *four* "complete diagrams," as shown in Fig. 2. By "complete diagrams" we mean the diagrams where the role of the white dots is explicitly demonstrated. Remembering that the white dots represent the creation or destruction of core holes or Auger electrons, it is easy to see how the zero-order diagram depicted by the left member of Fig. 2 corresponds to four complete diagrams shown on the right-hand side of the figure. In this diagram the downward-directed double lines and the thick single lines represent the core holes and Auger electrons, respectively. Since the transition matrix element $W_{\vec{k}\vec{p}\vec{p}'}$ is taken to be constant, these four diagrams contribute the same expression multiplied by the factors 2, 2, −1, and −1, respectively. The factors 2 and −1 occur due to summation over spins and exchange effects, respectively. Thus as far as the calculation of Auger intensity is concerned, it is unnecessary to know whether a white dot is connected to a core-hole line or an Auger line. The only relevant diagrams to consider then are those shown in Fig. 1 or in the left-hand side of Fig. 2. This was exactly what was done by NJ.

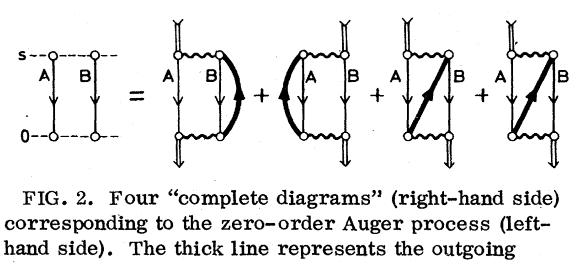

FIG. 2. Four "complete diagrams" (right-hand side) corresponding to the zero-order Auger process (left-hand side). The thick line represents the outgoing Auger electron.

The correlation function $\mathfrak{F}(s)$ as shown in Fig. 1 can be expressed as

$$\mathfrak{F}(s) = F_A(s)F_B(s)F_C(s)/F_D \quad ,$$

where the terms F_A, F_B, and F_C represent the contributions of the parts A, B, and C, respectively, and $F_D \equiv \langle\Phi_B|U(\infty, -\infty)|\Phi_B\rangle$ corresponds to the contribution from the denominator of Eq. (8). Note that $F_A(s) = F_B(s)$ (see Fig. 2) and that the denominator F_D would be equal to unity if the individual electronic states appearing in Eq. (4a) were described by scattered wave functions—the true eigenstates of $H_0 + H'$. In the real space there is an attractive potential due to the absence of an electron in the core state. Thus due to our choice of plane waves for the conduction electrons, the denominator can no longer be taken to be unity. In fact, it is found that both F_D in the denominator and $F_C(s)$ in the numerator become divergent in the presence of the many-body interaction term H'. This point has been discussed extensively in previous papers,[9,12] and it has been shown that the divergences of $F_C(s)$ and F_D cancel each other. One can appreciate this point rather easily as soon as one realizes that $F_C(s)$ and F_D are both vacuum contributions, and according to linked-cluster theorem one has $F_D = F_C(0)$. Let us then express $\mathfrak{F}(s)$ as

$$\mathfrak{F}(s) = \mathfrak{F}_A(s)\mathfrak{F}_C(s) \,, \tag{9}$$

where the first factor

$$\mathfrak{F}_A(s) = [F_A(s)]^2 \,, \tag{10}$$

corresponding to the open-line part of the ND-NJ problem, and the second term

$$\mathfrak{F}_C(s) = F_C(s)/F_C(0) \,, \tag{11}$$

corresponding to the closed-loop part. According to ND-NJ, in the edge region one has

$$\mathfrak{F}_A(s) = [(A/is)(i\xi_0 s)^{2\delta_0/\pi} e^{i\epsilon_0 s}]^2 \tag{12}$$

and

$$\mathfrak{F}_C(s) = (i\zeta_0 s)^\sigma \,, \tag{13}$$

with

$$\sigma = -2\sum_{l=0}^{\infty} 2(2l+1)(\delta_l/\pi)^2 \,. \tag{14}$$

Using Eq. (7) and formula

$$\frac{1}{\pi}\,\mathrm{Re}\int_0^\infty ds\,(is)^\lambda e^{i\epsilon s} = [\Gamma(-\lambda)\epsilon^{\lambda+1}]^{-1} \,,$$

one obtains from Eqs. (9), (12), and (13)

$$I(\omega \sim 2\epsilon_0) = \frac{A^2\epsilon}{\Gamma(2 - 4\delta_0/\pi - \sigma)}\left(\frac{\xi_0}{\epsilon}\right)^{4\delta_0/\pi}\left(\frac{\zeta_0}{\epsilon}\right)^\sigma \,, \tag{15}$$

where $\epsilon = 2\epsilon_0 - \omega \geq 0$. Thus we see that near the edge region the intensity $I(\omega \sim 2\epsilon_0)$ is given by a power of ϵ, where the exponent is $-(4\delta_0/\pi + \sigma - 1)$. This power-law behavior of the Auger intensity is in agreement with the result of NJ.

One notes that if the edge effects are neglected ($H' = 0$), one has

$$\mathfrak{F}_A^0(s) = [A(is)^{-1}e^{i\epsilon_0 s}]^2 ,$$

$$\mathfrak{F}_C^0(s) = 1 \,,$$

which give

$$I^0(\omega \sim 2\epsilon_0) = A^2\epsilon \,. \tag{16}$$

This zero-order approximation of Eq. (15) is in agreement with the well-known shape of Auger-band spectra,[13] *in the edge region*, obtained by the self-convolution of the Fermi distribution which in this region can be described by a simple step function. Since expressions (12)–(16) are provided by the ND-NJ theories, ξ_0 and ζ_0 appear as constants which are only estimated to be on the order of the Fermi energy. (Moreover, ND-NJ assume $\xi_0 = \zeta_0$.) They cannot be calculated explicitly since the scattering in these theories is described by a formal separable potential.

In this paper ξ_0 and ζ_0 will be replaced by energy-dependent functions, since the aim of the present paper is to extend the ND-NJ theory to energies well below the emission edge, and to determine the position of the Auger maximum. We propose to express Eq. (15) in the form

$$I(\omega) = I_A(\omega)I_C(\omega) \,, \tag{17}$$

such that for $\omega \sim 2\epsilon_0$ one has

$$I_A(\omega \sim 2\epsilon_0) = A^2\epsilon\left(\frac{\xi_0}{\epsilon}\right)^{4\delta_0/\pi} \tag{18}$$

and

$$I_C(\omega \sim 2\epsilon_0) = \left(\frac{\zeta_0}{\epsilon}\right)^\sigma \Big/ \Gamma\left(2 - \frac{4\delta_0}{\pi} - \sigma\right) . \tag{19}$$

The intensity $I(\omega)$ is thus factorized into two factors $I_A(\omega)$ and $I_C(\omega)$, where $I_A(\omega)$ is *essentially* related to the open-line part and $I_C(\omega)$ takes into account the contribution from the closed-loop part. Let us now express these factors in more elaborate forms.

In the present Auger problem the open-line part $I_A(\omega)$ contains two lines as shown in Fig. 1, whereas in the corresponding x-ray problem the open-line part contains only one open line. We can thus write

$$I_A(\omega) = \int d\omega_1 \int d\omega_2\, \delta(\omega - \omega_1 - \omega_2) I_X(\omega_1) I_X(\omega_2) \,, \tag{20}$$

where $I_X(\omega)$ is similar to the open-line part of the x-ray problem. In Ref. 6, $I_X(\omega)$ was given in the form

$$I_X(\omega) = J(\omega)G(\omega)[\xi(\omega)/\epsilon_0 - \omega]^{2\delta_0/\pi} . \qquad (21)$$

Such an expression will be used in Eq. (20). The function $J(\omega)$ ($\propto\omega^{1/2}$) represents the state density with a sharp cutoff at $\omega = \epsilon_0$. A zero-order calculation of Eq. (20) can be performed using the diagrammatic rules of the Appendix, and yields

$$I_A^0(\omega) = \frac{\pi W^4}{4}\int_0^{\epsilon_0} d\omega_1 \int_0^{\epsilon_0} d\omega_2\, \delta(\omega - \omega_1 - \omega_2) \times (\omega_1\omega_2)^{1/2} . \qquad (22)$$

Thus we can write $J(\omega)$ explicitly as

$$J(\omega) = \tfrac{1}{2}(\pi^{1/2}W^2)\omega^{1/2}\theta(\epsilon_0 - \omega) , \qquad (23)$$

where θ is the step function. The function $G(\omega)$ in Eq. (21) takes into account the difference in the nature of the black- and white-dot vertices which represent the electron-core-hole interactions, and the production of Auger electrons, respectively. The difference in the momentum dependence of these vertices as shown by Eqs. (5) and (6) [see also (A2)] was neglected by ND-NJ. However, retention of this momentum dependence gives rise to the factor $G(\omega)$, the detailed nature of which will be discussed in Sec. IV. Constant factor A appearing in Eq. (18) can be obtained by calculating Eq. (22) in the edge region. One has

$$I_A^0(\omega \sim 2\epsilon_0) = \tfrac{1}{4}(\pi W^4)\epsilon_0(2\epsilon_0 - \omega) .$$

Hence, according to Eq. (16), $A^2 = \tfrac{1}{4}(\pi W^4\epsilon_0)$.

The factor $I_C(\omega)$ of Eq. (17), corresponding to the correction due to the closed-loop part of Fig. 1, can be expressed in the form

$$I_C(\omega) = [\zeta(\omega)/(2\epsilon_0 - \omega)]^{\sigma} . \qquad (24)$$

The functions $\xi(\omega)$, $\zeta(\omega)$, and $G(\omega)$ appearing in Eqs. (21) and (24) will have the limiting values of ξ_0, ζ_0, and 1, respectively, in agreement with Eqs. (18) and (19). [The constant denominator Γ appearing in Eq. (19) is very close to 1. It will be considered as being absorbed in $\zeta(\omega)$]. Let us note that our choice of expressing our results in the forms of Eqs. (21) and (24) is more formal than physical. For instance, we could have chosen ξ and ζ as constants, in which case the exponents δ_0 and σ would be ω dependent.

The spirit of the calculation of the Auger intensity (17) is the same as that of the calculation of the x-ray intensity as presented in Ref. 6. The calculation in Ref. 6 is such that in the low-energy region ($\omega \lesssim 0$), it reproduces the results of the calculation obtained from a first-order theory in the electron-electron and electron–core-hole effective interactions. Such an approximation is quite satisfactory since it adequately describes the low-energy features of the x-ray emission-band spectra (tailing and plasmon satellite).[9] There is no reason to believe that our theory will not work as well in describing the low-energy intrinsic features of the Auger spectra, the physical situations being quite similar.[14]

The first-order diagrams corresponding to Auger emission are contained in the general diagrams of Fig. 1. In this case, the open lines would contain zero and/or one black dot, and in those cases where the closed loops appear, they would contain two black dots. (The two vertex loops are the lowest-order loops giving a nonzero contribution.)

The basic requirement to extend the ND-NJ theory beyond the immediate neighborhood of the emission edge is the use of a *realistic nonseparable potential.* The above mentioned first-order theory allows us to introduce a realistic core-hole potential. However, in the edge region, this theory gives Eqs. (21) and (24) in the form

$$I_X(\omega) = J(\omega)G(\omega)\{1 + 4\delta_0^B/\pi \ln[\xi(\omega)/(\epsilon_0 - \omega)]\} \qquad (25)$$

and

$$I_C(\omega) = 1 + \sigma^B \ln[\zeta(\omega)/(2\epsilon_0 - \omega)] , \qquad (26)$$

where the phase shift δ_0^B, as indicated by the superscript B, is calculated in the Born approximation. As discussed in Sec. IV of Ref. 6, the Born phase shifts satisfy the Friedel sum rule exactly and can be considered to be satisfactory approximations of the actual phase shifts (the relative error is never more than 10%).

The program in Secs. III and IV will be to evaluate $\xi(\omega)$ and $\zeta(\omega)$ by using the first-order theory, i.e., to calculate Eqs. (25) and (26). Then we will use these functions to evaluate $I_X(\omega)$ and $I_C(\omega)$ according to Eqs. (21) and (24), and, finally, obtain the Auger intensity from Eqs. (17) and (20). Such a scheme will give results which will automatically satisfy the ND-NJ asymptotic expression (15) in the edge region.

III. CLOSED-LOOP CONTRIBUTION

Since $F_C(s)$ in Eq. (11) is a vacuum contribution, it can be written in the form $F_C(s) = e^{C(s)}$. Equation (9) then takes the form

$$\mathfrak{F}(s) = \mathfrak{F}_A(s)\exp[C(s) - C(0)] , \qquad (27)$$

where $C(s)$ is the sum of all the linked vacuum loops. In the lowest significant order of the core-hole potential, Eq. (27) becomes

$$\mathfrak{F}(s) = \mathfrak{F}_A(s)[1 + C_2(s) - C_2(0)] , \qquad (28)$$

where we have included the contributions from only two vertex loops. This corresponds to calculating the phase shifts in Born approximation.

Expression (28) is then calculated by using the diagrammatic rules given in the Appendix. One obtains

$$C_2(s) - C_2(0) = -\int_{k_0}^{\infty} dp \int_0^{k_0} dq \frac{4pq\sigma(p,q)}{(p^2-q^2)^2} \int dt_1 \int dt_2 \exp[i(p^2-q^2)(t_1-t_2)], \tag{29}$$

where the domain of integration of (t_1, t_2) is $(0 < t_1 < s$ or $0 < t_2 < s$, and $t_1 < t_2)$. The function $\sigma(p,q)$ is defined in the Appendix and one has $\sigma(k_0, k_0) = \sigma$ given by Eq. (14). After performing the t integrations in Eq. (29) and dropping the terms proportional to s, which only produce a band shift irrelevant to the present problem, we substitute Eq. (28) in Eq. (7) to obtain

$$I(\omega) = I_A(\omega)[1 + Z(\omega)], \tag{30}$$

with

$$Z(\omega) = \int_{k_0}^{\infty} dp \int_0^{k_0} dq \frac{4pq\sigma(p,q)}{(p^2-q^2)^2} \times \left(1 - \frac{I^0(\omega + p^2 - q^2)}{I^0(\omega)}\right), \tag{31}$$

where we have replaced I_A by I^0 on the right-hand side of Eq. (31). This approximation can be made in $Z(\omega)$, since it only introduces higher-order corrections. The function $Z(\omega)$ is similar to function $E(\omega)$ introduced in Sec. III of Ref. 6. The only difference is that I^0 is now given by Eq. (22) instead of the free-electron density of states.

The double integration of Eq. (31) is performed numerically to obtain $Z(\omega)$. Once $Z(\omega)$ is computed, Eq. (30) can be recast in the exponential form

$$I(\omega) = I_A(\omega) e^{Z(\omega)}, \tag{32}$$

as was done in Ref. 6. Thus the closed-loop contribution to Auger intensity is

$$I_C(\omega) = e^{Z(\omega)}. \tag{33}$$

$I_C(\omega)$ can also be expressed in the form of Eq. (24) by expressing $\zeta(\omega)$ as

$$\zeta(\omega) = (2\epsilon_0 - \omega) e^{Z(\omega)/\sigma}. \tag{34}$$

The next step will be the calculation of $I_A(\omega)$, which will be carried out in Sec. IV. However, before proceeding with such a calculation let us show that Eq. (33) recovers the correct ND-NJ power $\zeta_0/(2\epsilon_0 - \omega)^\sigma$ for the closed-loop contribution in the edge region ($\omega \lesssim 2\epsilon_0$). In other words, we want to show that $\zeta(\omega)$ given by Eq. (34) is a smooth function of ω in the edge region.

In the edge region I^0, appearing in Eq. (31), has a finite discontinuity in its slope, in that the slope is finite for $\omega < 2\epsilon_0$ and zero for $\omega > 2\epsilon_0$, and can be written

$$I_0(\omega) = (2\epsilon_0 - \omega) C(\omega) \theta(2\epsilon_0 - \omega).$$

$C(\omega)$ is a smooth function for $\omega \approx 2\epsilon_0$. For $\omega \lesssim 2\epsilon_0$ (or for $\epsilon = 2\epsilon_0 - \omega$ small), $Z(\omega)$ given by Eq. (31) can be written

$$Z(\omega \sim 2\epsilon_0) = \frac{\sigma}{\epsilon} \iint_a dp\, dq \frac{4pq}{p^2 - q^2} + \sigma \iint_A dp\, dq \frac{4pq}{(p^2-q^2)^2} + \iint dp\, dq \frac{4pq}{(p^2-q^2)^2} [\sigma(p,q) - \sigma], \tag{35}$$

where the areas of integration a and A are depicted in Fig. 3. Area a vanishes when ϵ tends to zero. The integrals of the first two terms of Eq. (35) can be performed exactly, and the third integral does not diverge when ϵ tends to zero. Its domain A can thus be replaced by $A + a$. These considerations lead Eq. (35) to

$$Z(\omega \sim 2\epsilon_0) = \sigma[L + \ln(\epsilon_0/(2\epsilon_0 - \omega))],$$

with

$$L = 2 + \int_{k_0}^{\infty} dp \int_0^{k_0} dq \frac{4pq}{p^2 - q^2} \left(\frac{\sigma(p,q)}{\sigma} - 1\right),$$

which is a finite constant, and from Eq. (34) one obtains

$$\zeta_0 = \epsilon_0 e^L,$$

which is also finite.

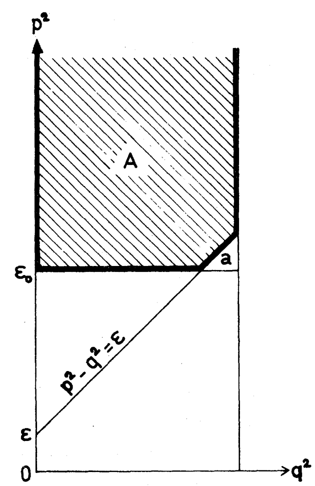

FIG. 3. Regions of integration (A and a) for the evaluation of the function $Z(\omega)$ by using Eq. (35). Area a vanishes when ω tends to $2\epsilon_0$.

IV. OPEN-LINE CONTRIBUTION

As shown by Eqs. (10) and (20), the total open-line contribution appears as the convolution of two single-line contributions. As it has been discussed in Sec. II, the single-line intensity $I_X(\omega)$, which must be self-convoluted, can be written in the form of Eq. (21) as

$$I_X(\omega) = J(\omega)G(\omega)[\xi(\omega)/(\epsilon_0-\omega)]^{2\delta_0/\pi} . \qquad (36)$$

Our task now is to determine the function $\xi(\omega)$ and $G(\omega)$. The intensity $I_X(\omega)$ is obtained from

$$I_X(\omega) = \frac{1}{\pi}\,\mathrm{Re}\int_0^\infty ds\, e^{-i\omega s}F_A(s) , \qquad (37)$$

where $F_A(s)$, appearing in Eq. (8), can be evaluated by using the diagrammatic rules given in the Appendix. The method of this calculation is very similar to that discussed in Sec. V of Ref. 6.

Because of the presence of two distinct vertices corresponding to the Auger collision (destruction of the core hole and production of the Auger electron), and the scattering by the core-hole potential, the calculation of $I_X(\omega)$ is somewhat more difficult than the closed-loop calculation of Sec. III. Each Auger vertex (white dot in Fig. 1) contributes a constant factor W [see Eq. (6)], whereas each scattering vertex (black dot) contributes a factor $iD_0(p,p')$ [see Eq. (A2)]. If both vertex functions had the same momentum dependence, $G(\omega)$ in Eq. (36) would be equal to unity. However, because of the difference in the nature of these two vertices, G becomes a slowly varying function of ω except near the Fermi edge ($\omega=\epsilon_0$), where it has a singular slope,[15] i.e.,

$$G(\epsilon_0)=1 \text{ and } (dG/d\omega)_{\omega=\epsilon_0}=\infty .$$

For the details of the calculation of $I_X(\omega)$, we refer to Sec. V of Ref. 6. There are, however, two points of departure which should be mentioned at this stage. First, in this paper we consider only the $l=0$ case, or, in other words, the white-dot vertex, which in Ref. 6 is related to a dipolar matrix element proportional to p^l, is now replaced by constant W. The second point is formal. The function $G(\omega)$ of the present paper is the same as $G(\omega)$ of Ref. 6 multiplied by $[\xi(\omega)]^{2\delta_0/\pi}$, i.e., Eq. (53) of Ref. 6 is now replaced by

$$G(\omega) = A(\omega)[\xi(\omega)]^{2\delta_0/\pi} + B(\omega)(\epsilon_0-\omega)^{2\delta_0/\pi}$$

(ξ_0 of Ref. 6 is called ξ here). The rest of the calculation is quite similar to the one for the closed-loop part. The following set of equations are parallel to Eqs. (30)–(32) and (34):

$$I_X(\omega) = J(\omega)G(\omega)[1+E(\omega)] , \qquad (30')$$

with

$$E(\omega) = \int dp \int dq\, \frac{4pq\sigma_0(p,q)}{(p^2-q^2)^2}\left(1-\frac{J(\omega+p^2-q^2)}{J(\omega)}\right) . \qquad (31')$$

Next, $I_X(\omega)$ is expressed in the exponential form

$$I_X(\omega) = J(\omega)G(\omega)e^{E(\omega)} , \qquad (32')$$

which can be written in the form of a power law

$$I_X(\omega) = J(\omega)G(\omega)[\xi(\omega)/(\epsilon_0-\omega)]^{2\delta_0/\pi}$$

by defining

$$\xi(\omega) = (\epsilon_0-\omega)\, e^{E(\omega)/\sigma} . \qquad (34')$$

[Function $\sigma_0(p,q)$ is defined in the Appendix.] Like $\zeta(\omega)$, $\xi(\omega)$ can be shown to have a nonsingular behavior for $\omega=\epsilon_0$.

V. RESULTS AND DISCUSSIONS

In this paper we have extended the ND-NJ edge theory to energies well below the emission edge, in order to study the effect of excitations of weak-energy electron-hole pairs on the CVV Auger spectra of metals. This has been accomplished by the introduction of a realistic nonseparable pseudopotential to describe the scattering of the conduction electrons by the initial hole in the core state. Use of such a realistic pseudopotential necessitated introduction of approximations in calculating the electron phase shifts at the Fermi level. The phase shifts have been calculated in Born approximation and have been found to satisfy Friedel sum rule and to be in good agreement with other calculations.

The only observable effect of the extended ND-NJ edge-anomaly theory is the shift in the position of the Auger intensity maximum. Numerical calculations have been carried out for the $L_{23}VV$ Auger spectra of Al, and the results are shown in Fig. 4. The dashed curve represents the one electron Auger band obtained by the self-convolution of the free-electron density of state function proportional to $\omega^{1/2}$. This zero-order curve is expected to be modified once the many-body effects are introduced. A very crude method of incorporating these many-body effects is a naive utilization the ND-NJ power law. As discussed in Sec. I, in this approach the Auger spectrum is calculated by multiplying the zero-order intensity by a factor $(\xi_0/\epsilon)^{\alpha_{A}+1}$ with a constant energy ξ_0. This yields the dotted curve of Fig. 4 where the Auger maximum is considerably shifted, bringing it closer to the experimental peak. However, since the ND-NJ power law is supposed to be valid very close to the emission edge, its utilization to obtain results at lower energies is unsatisfactory. We therefore proceeded to a more systematic ex-

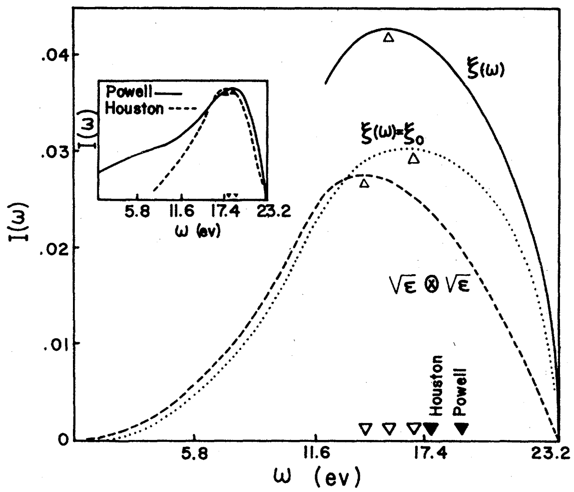

FIG. 4. Line shapes for the $L_{23}VV$ Auger spectrum of Al. The dashed curve representing the one-electron band shape is plotted as a reference for comparison. The dotted curve is obtained by multiplying the one-electron curve with the NJ power-law factor. The solid curve is the result of the present calculation. The inset shows the experimental profiles of Powell and Houston.

tension of the edge theory to lower energies as presented in Sec. I–IV of the present paper. The final Auger-band intensity obtained from Eqs. (17), (20), (21), and (24) is shown by the solid curve of Fig. 4. The relative intensities of the various curves in this figure are irrelevant from experimental point of view since absolute intensities cannot be measured. The only point to emphasize in this figure is the shift in the position of the Auger maximum. The calculated positions of the maximum are shown by the white triangles, whereas the experimental peaks as obtained by Powell and Houston are shown by the black triangles. The full experimental curves are shown in the inset. Powell's curve is a result of subtracting a plausible but arbitrary background from the raw data. Houston has used a dynamic background subtraction technique to subtract the contribution of the secondary electrons. This difference in the background subtraction technique may be responsible for the occurrence of their Auger peaks at two different energies. A satisfactory resolution of this difference would be helpful in comparing the theoretical result with experiment. In any case, the shift of the Auger peak as obtained from our extended edge theory is smaller than that of the aforementioned calculation utilizing the ND-NJ power law. In our theory $\xi(\omega)$ [and the other functions like $\zeta(\omega)$ and $G(\omega)$] is energy dependent. The energy dependence of these functions attenuates the effect of the anomalous ND-NJ power-law behavior with constant ξ_0.

Several other effects, not considered in this paper, can also modify the Auger line shape. First, the energy dependence of the transition matrix element in the free-electron gas model has been considered by several authors.[4,10,16] These calculations show that the matrix element is very weakly dependent on energy and does not introduce any appreciable shift in the position of the Auger peak. However, an evaluation of the Auger matrix element for Al with more realistic wave function[17] for the conduction electron and the core state is yet to be carried out, and this may modify the Auger line shape. In several recent studies[18] of the s-p materials such as silicon, the Auger matrix element has been found to be dependent on the local angular momentum of the final state holes. Whether this effect will also modify the Auger line shape of a metal like Al is a matter of further study. Since the mean free path of an Auger electron in a metal is only 3–4 Å, the electrons which are ejected from the surface must originate very close to the surface. Thus the surface effects may play a role in altering the Auger line shape. The surface effects on the Auger spectra of metals have been considered by several authors.[16,19,20] The peak shift obtained by these authors is of correct sign but it is not significant in magnitude. However, to our knowledge, a self-consistent theory of the surface effects on the Auger spectra of metals has not been proposed yet.

In this paper we have essentially considered the effect of the weak-energy pair production due to scattering by the initial core hole on the high-energy region of the CVV Auger spectra of metals. Other many-body effects such as the intraband interactions among the conduction electrons[9,21] have not been included, since they are known to modify the one electron band shape only in the low-energy region. In particular, when these intraband interactions are considered along with the scattering of the conduction electrons by the initial core hole, the Auger and the x-ray spectra of a metal develop tailing and a secondary maximum at these low energies. The tailing is the effect of the individual electron-hole pair creation by the intraband electron-electron interactions. The low-energy secondary maximum occurs due to the simultaneous generation of a plasmon in the medium. The effect of plasmon production and the low-energy behavior of the x-ray and Auger spectra of metals have been discussed by various authors.[9–12,21] These effects, however, do not play any essential role on the intensity in the high-energy region[11] and, in particular, in modifying the position of the main peak of the Auger spectrum.

ACKNOWLEDGMENTS

This research has been supported in part by the NATO Research Grant No. 1433, and ESIS, Universities of Liège and Antwerp, Belgium.

APPENDIX

Since the energy involved in an Auger collision is large compared to the Fermi energy, such a collision occurs in a small region whose range is on the order of the core-hole radius. On the other hand, since the core radius is smaller than the conduction-electron wave length, mainly the s-wave part ($l=0$) of the conduction-electron wave function will contribute to the Auger process. Thus this is the only partial wave which appears in the open-line part of our problem. For the closed-loop part, however, one has to sum over all partial waves (and spins).

Since we use the pseudopotential approach, the conduction electrons are described by plane waves. The core-hole scattering potential can then be written

$$V_{\vec{p}\vec{p}'}=\sum_{l=0}^{\infty} Y_l^m(\hat{p})Y_l^m(\hat{p}')D_l(p,p'), \tag{A1}$$

with

$$D_l(p,p')=(4\pi^2pp')^{-1}\times\int_{|\vec{p}-\vec{p}'|}^{p+p'} dq\, q\, V(q)P_l\left(\frac{p^2+p'^2-q^2}{2pp'}\right) \tag{A2}$$

and

$$V(q)=V_{\text{ps}}(q)/\epsilon(q)\ . \tag{A3}$$

The Born phase shifts at the Fermi level are related to these functions by

$$\delta_l=\tfrac{1}{2}\pi k_0 D_l(k_0,k_0)\ . \tag{A4}$$

The functions $\sigma_l(p,p')$ and $\sigma(p,p)$ appearing in the calculation are defined as

$$\sigma_l(p,p')=-\tfrac{1}{2}pp'[D_l(p,p')]^2 \tag{A5}$$

and

$$\sigma(p,p')=\sum_{l=0}^{\infty}\sigma_l(p,p'), \tag{A6}$$

$$=-(2\pi)^{-4}\int_{|\vec{p}-\vec{p}'|}^{p+p'} dq\, q[V(q)]^2\ , \tag{A7}$$

whose value

$$\sigma\equiv\sigma(k_0,k_0)$$

at the Fermi level is the exponent of the closed-loop part of the edge effect.

Let us now enumerate the rules for evaluating the diagrams corresponding to the function $F(s)$. An Auger vertex (white dot) contributes by a factor W and a scattering vertex (black dot) contributes by a factor $iD_l(p,p')$ (use only $l=0$ for the open-line part). The contribution of a particle line ($p>k_0$) is given by $p^2\exp[ip^2(t_1-t_2)]$ and that of a hole line ($p<k_0$) is $-p^2\exp[ip^2(t_1-t_2)]$ (lines run from t_1 to t_2). A factor $-2l(l+1)$ appears for every closed loop. One sums over all l's and integrates over all momenta p and time t. For more details regarding the *diagrammatic rules* we refer to Appendices B and C of Ref. 6.

Finally, we present an explicit evaluation of the pseudopotential used in this paper. We use the Ashcroft pseudopotential[22] which is Coulombic beyond a cut-off radius R_c and is zero within this radius because of the core effects. In momentum space this pseudopotential takes a rather simple form:

$$V_{\text{ps}}(q)=(4\pi e^2/q^2)\cos(qR_c)\ . \tag{A8}$$

Ashcroft has proposed the values of the cut-off radius R_c for a series of metals, including Al, in which we are particularly interested in the present paper. However, the R_c values given by Ashcroft are evaluated only for the normal ions of the metals and cannot be used for those ions which have one electron missing in the core state, as is the case for the ions involved in an Auger transition. However, according to an argument proposed by Ashcroft[23] and developed in Sec. IV of Ref. 6, there is a proportionality rule between the Ashcroft R_c and the radius of the valence orbital of the neutral atom. Since the radii of the valence orbital of a neutral and ionized atom can be evaluated by using the Slater rules,[24] one can calculate the Ashcroft radius R_c^* of an ionized atom by knowing R_c and by using the proportionality rule.

According to Ashcroft the cut-off radius for the metallic ion of Al is $R_c=0.59$ Å $=1.115$ a.u. The corresponding free atom is in the electronic state $1s^2 2(\text{sp})^8 3(\text{sp})^3$ and according to Slater rules, its valence orbital has the radius $R_{\text{Sl}}=0.857$ a.u. If a $2p$ core hole is created in this free atom, it would be in the state $(1s)^2 2(\text{sp})^7 3(\text{sp})^3$. The valence-orbital radius of such an ionized atom will, according to Slater rules, be found to have a smaller radius of $R_{\text{Sl}}^*=0.690$ a.u. Then using the proportionality rule, we obtain $R_c^*=0.897$ a.u. This numerical value has been used for the cut-off radius in Eq. (A8) and all the numerical calculations of this paper.

[1]G. D. Mahan, Phys. Rev. 163, 612 (1967).

[2]P. Nozières and C. T. deDominicis, Phys. Rev. 178, 1097 (1969).

[3]S. Doniach and M. Šunjić, J. Phys. C 3, 285 (1970).

[4]M. Natta and P. Joyes, J. Phys. Chem. Solids 31, 447 (1970).

[5]G. A. Ausman and A. J. Glick, Phys. Rev. 183, 687 (1969).

[6]P. Longe, Phys. Rev. B 8, 2572 (1973).

[7]C. J. Powell, Phys. Rev. Lett. 30, 1179 (1973).

[8]J. E. Houston, J. Vac. Sci. Technol. 12, 255 (1974).

[9]B. Bergersen, F. Brouers, and P. Longe, J. Phys. F 1, 945 (1971).

[10]A. L. Hagen and A. J. Glick, Phys. Rev. B 13, 1580 (1976).

[11]S. M. Bose and J. Fitchek, Phys. Lett. A 48, 443 (1974); J. Fitchek and S. M. Bose, Phys. Lett. A 54, 460 (1975).

[12]S. M. Bose and A. J. Glick, Phys. Rev. B 17, 2073 (1978).

[13]J. J. Lander, Phys. Rev. 91, 1382 (1953).

[14]Such a calculation could be performed in the framework of the present investigation. This will only give the intrinsic contributions to the Auger intensity due to many-body effects. The observed spectra are, however, a superposition of these intrinsic features as well as the extrinsic features occurring due to energy loss by the Auger electron by inelastic collisions on its way to the metal surface. Thus our computation of the intrinsic features will not yield any easy comparison with experiment at least at the low-energy side of the Auger spectra and as such we refrain from undertaking such a calculation in the present paper.

[15]P. Longe, Phys. Rev. B 10, 529 (1974).

[16]A. J. Jackson, C. Tate, T. E. Gallon, P. J. Bassett, and J. A. D. Mathew, J. Phys. F 5, 363 (1975).

[17]D. W. Jennison, Phys. Rev. Lett 40, 807 (1978); Bull. Am. Phys. Soc. 23, 334 (1978).

[18]P. J. Feibelman, E. J. McGuire, and K. C. Pandey, Phys. Rev. B 15, 2202 (1977); P. J. Feibelman and E. J. McGuire, *ibid.* 17, 690 (1978).

[19]J. W. Gadzuk, Phys. Rev. B 9, 1978 (1974).

[20]S. M. Bose and E-Ni Foo (unpublished).

[21]S. M. Bose and A. J. Glick, Phys. Rev. B 10, 2733 (1974).

[22]N. W. Ashcroft, Phys. Lett. 23, 48 (1966); J. Phys. C 1, 232 (1968).

[23]N. W. Ashcroft, in *Soft X-Ray Band Spectra*, edited by D. J. Fabian (Academic, New York, 1968), p. 259.

[24]J. C. Slater, Phys. Rev. 36, 57 (1930).